

Title

Diffusion Tensor Imaging: *In Vivo* White Matter Structural and Connectivity Evaluation of Glioma Pathophysiology for Future Clinical Application

By

Shawn D'Souza

Department of Psychology and Neuroscience | University of Colorado: Boulder

Defense Date:

April 2nd, 2019

Thesis Advisor:

John A. Thompson, Ph.D., Department of Neurosurgery | University of Colorado: Anschutz Medical Campus

Honor Council Representative:

Akira Miyake, Ph.D., Department of Psychology and Neuroscience | University of Colorado: Boulder

Third Committee Member:

Nancy A. Guild, Ph.D., Department of Molecular, Cellular and Developmental Biology | University of Colorado: Boulder

Fourth Committee Member:

Alison Vigers, Ph.D., Department of Psychology and Neuroscience | University of Colorado: Boulder

Table of Contents

Abstract.....	4
Introduction.....	5
Background.....	5
Objectives.....	6
Diffusion Tensor Imaging.....	7
Along-Tract-Analysis.....	7
Major white matter pathways.....	8
Experimental Groups for ATA.....	8
Connectometry.....	8
Hypothesis.....	9
Methodology.....	10
Population Selection.....	10
Imaging Sequence Parameters.....	12
Pre-processing.....	12
Tumor Segmentation.....	12
ITK-Snap Segmentation registration to DTI Image Space.....	13
DSI Studio Streamline Deterministic Fiber Tracking.....	13
Hemispheric ROI and tractography constructions and analysis.....	14
Targeted white matter bundle reconstruction.....	14
Volumetric Analysis.....	15
Lobe localization Analysis.....	15
Along-Tract-Analysis.....	16
Structural Connectometry.....	16
Results.....	16
Objective 1: Glioma impact on hemispheric tractography.....	16
Objective 2: Glioma grade and metastasis impact on white matter integrity.....	17
Objective 3: Tumor volumetric correlation.....	18

Objective 4: Glioma lobe localization and its effect on the SLF and CST.....	18
Objective 5: Impact of glioma proximity on white matter integrity of CST and SLF.....	18
Objective 6: Glioma impact on structural connectivity.....	20
Discussion.....	20
Broader Impacts.....	24
Limitations.....	26
References.....	28
Appendices.....	31
Figure legends.....	31

Abstract:

Gliomas account for 26.5% of all primary central nervous system tumors. Histopathological observation has been the gold standard for diagnosing and studying gliomas, however, this method has several limitations. Recent studies have used diffusion tensor imaging (DTI) to extract white matter fibers and the diffusion coefficients derived from the magnetic resonance processing to provide non-invasive insights into the extent of tumor invasion, axonal integrity, and pathophysiological differentiation of glioma from metastasis. This work extends the capabilities of DTI by examining whether a tract-based analysis can improve non-invasive localization of tumor impact on white matter integrity. This study also examines the anatomical shift gliomas may have on white matter by implementing a structural connectometry analysis. This study retrospectively analyzed preoperative MRIs highlighting pathological tissue through contrast enhancement and DTI scans of subjects that were biopsy confirmed to have either high or low-grade glioma. Whole-brain-seeding, required for structural connectometry and reconstruction of specific white matter pathways, was derived through DSI Studio's deterministic Euler Streamline Algorithm. Two major white matter pathways, the corticospinal tract and superior longitudinal fasciculus, were reconstructed for along-tract-analysis by applying atlas-based regions of interest. Ipsilesional and contralesional hemisphere tractography were used to compute within-subject comparisons for all analyses. Diffusion parameters indicated higher levels of white matter degradation in the ipsilesional hemisphere. Novel application of along-tract-analysis revealed tracts traversing the tumor region showed significant white matter degradation which decreased with distance from the tumor. Furthermore, connectometry revealed a shift in anatomical connections of the ipsilesional compared to the contralesional hemisphere.

Introduction:

Background:

Gliomas are a devastating cancer, accounting for 27% of all brain tumors and 80% of all malignant tumors (Ostrom *et al.*, 2018). This cancer originates from the astrocytes, oligodendrocytes, and ependymal cells of the brain (Louis *et al.*, 2016). Symptoms can range from cellular degradation to psychological damage including necrosis, hypoxia, structural epilepsy, and cognitive impairment (Goldbrunner *et al.*, 2018; Raza *et al.*, 2002). Limited and often deleterious treatment options, including chemotherapy and radiotherapy, contribute to poor prognosis. Surgical resection remains the quickest and most effective option to remove a substantial portion of cancerous tissue (Hervy-Jumper *et al.*, 2014, Johns Hopkins Glioma Center). However, this route presents significant risk for patients including mental and emotional stress as well as potential damage to functional brain circuitry. Preserving brain function in resection cases is challenging due to difficulty in clearly identifying the boundary between cancerous and normal tissue.

In addition, histopathological observation and biochemical manipulation have been the gold standard for diagnosing and studying gliomas respectively (Deighton *et al.*, 2010). However, these methods depend on biopsy, another invasive surgical technique which extracts a tumor tissue sample from the patient's brain. Furthermore, the visual depth afforded by histopathology is limited to the plane from which the cell sample was extracted.

These challenges show the need for a non-invasive method of 3D visualization of functional brain tractography to better define and study glioma pathophysiology on surrounding

white matter milieu. In this study, we sought to determine the efficacy of using diffusion tensor imaging parameters for describing tumor invasion in the brain.

Objectives:

This study aims to explore DTI's capability of non-invasively exploring glioma pathophysiology on white matter integrity to address the challenges mentioned above. The four primary diffusion parameters reported in the literature are associated with features of axonal integrity: Radial Diffusivity (RD), Axial Diffusivity (AD), Mean Diffusivity (MD), and Fractional Anisotropy (FA). RD and AD measure the magnitude of water diffusion perpendicular and parallel to the axon, respectively. These, in turn, indirectly measure axonal integrity. MD indirectly measures myelination by quantifying radial water diffusion restriction. Finally, FA quantifies magnitude and directionality of water diffusion, indirectly measuring the efficiency of white matter physiological activity (Ormond *et al.*, 2017, Alexander *et al.*, 2007). Literature has shown that higher levels of RD/MD and lower levels of AD/FA are indicative of reduced myelination and axonal structural integrity (Winklewski *et al.*, 2018, Clark *et al.*, 2011, Alexander *et al.*, 2007, Song *et al.*, 2003). Unique application of these diffusion parameters in hemispheric (ipsilesional versus contralesional) analysis, along-tract-analysis (ATA), and structural connectometry will be utilized to examine glioma pathophysiology on white matter integrity and neural circuitry. Six objectives will be addressed in this study:

Objective 1: Glioma impact on hemispheric tractography

Objective 2: Glioma grade and metastasis impact on white matter integrity

Objective 3: Tumor volumetric correlation

Objective 4: Glioma lobe localization and its effect on the SLF and CST

Objective 5: Impact of glioma proximity on white matter integrity of CST and SLF

Objective 6: Glioma impact on structural connectivity

Outlined below is background information on the tools and analyses that will be employed throughout the study to answer these objectives.

Diffusion Tensor Imaging:

DTI is an *in vivo* neuroimaging technique which measures anisotropic water diffusion to extract white matter tractography and produce the four quantitative diffusion parameters (Bucci *et al.*, 2013). Thus far, DTI has been utilized as a structural tool to improve pre- and intraoperative resection technique and preserve postoperative functionality. Preoperative imaging locates eloquent tracts at risk of damage during resection and confirms tumor regions of excision and avoidance (Essayed *et al.*, 2017). Preoperative imaging has also been used as a predictive tool to assess postresection morbidity and mortality (Caverzasi *et al.*, 2016; Meyer *et al.*, 2017). Intraoperative use allows for correction of intraoperative brain shift and increases spatial resolution of functional brain mapping techniques, such as direct electrical stimulation (D'Andrea *et al.*, 2016; Vassal *et al.*, 2013).

Along-Tract-Analysis:

Tract length varies between individual subjects. In addition, diffusion metrics change at different points along the length of a white matter fiber. To have a normalized comparison between all subjects and have a holistic tractographic analysis, ATA was utilized. This process calculates the mean length of the white matter pathway of interest across all subjects, followed by interpolation or down sampling each fiber to fit all subjects' tracts to the standard mean length (Colby *et al.*, 2012, Ormond *et al.*, 2017). The average diffusion metric is then calculated at each

point along the length of the normalized tract. This study applies ATA in a novel context to answer how tumor effect varies with distance.

Major White Matter Pathways:

ATA was run on two major white matter pathways: the Corticospinal Tract (CST), critical for voluntary movement (Natali and Bordoni, 2018), and the Superior Longitudinal Fasciculus (SLF), critical for motor coordination and speech function (Kamali *et al.*, 2014). The CST and SLF were chosen based on anatomy and significance in glioma resection cases. The CST extends from the cerebral cortex to the brain stem, providing a rostral - caudal measure (Natali and Bordoni, 2018). The SLF connects the major lobes of the cortex, providing an anterior - posterior measure (Kamali *et al.*, 2014). In addition, these pathways occupy a significant portion of the brain, putting them at risk for damage in supratentorial tumor cases from both the tumor and surgical intervention.

Experimental Groups for ATA:

To home in on tumor effect, subject tracts were segregated into three experimental groups: All tracts of the CST/SLF in the contralesional hemisphere (control) (C), tracts of the CST/SLF of the ipsilesional hemisphere which do not cross the tumor region of interest (Ipsilesional Exclusive)(IE), and tracts of the CST/SLF of the ipsilesional hemisphere which cross the tumor region of interest at some area along the length of the tract (Ipsilesional Inclusive)(II).

Connectometry:

The preservation of human brain function is of utmost priority in the neurosurgical field. With this goal comes the challenge of understanding the functional neuroanatomy of the human brain. As with complex networks in general, functionality is highly correlated to the physical

interactions between the network's unique components (Hagmann *et al.*, 2008). Application of graph-network theory algorithms to tractographic data permits estimates of brain connectometry and may shed light on the intricate anatomical interactions between specialized brain regions.

Previous studies have employed graph theory to represent the anatomical connections between one brain region to another (Hart *et al.*, 2016, Bullmore *et al.*, 2009). Graph theory visualizes networks through a series of nodes and edges. Nodes, in the context of neuroanatomy, are brain atlas derived regions of interest, which could represent gray matter, white matter or fMRI based information. Edges represent the relationship between one node and another, usually through a representative line, and in neuroanatomy often represent DTI tractography. Edge based analyses can encode several pieces of information including the strength or number of connections between one brain region to a another (encoded by line thickness) (Hart *et al.*, 2016).

Thus far, no studies have quantitatively analyzed how gliomas shift the anatomical connections of the brain. We aim to identify how structural brain connectometry differs between the contralesional and ipsilesional hemispheres of the subject population as well as compare the microstructural integrity of these connections through FA and MD analysis.

Hypothesis:

If histopathology and biochemical analysis has shown gliomas are capable of necrosis, breakdown of the blood brain barrier, and hypoxia of surrounding tissue, then DTI ATA of the CST and SLF will show higher signs of white matter degradation in ipsilesional inclusive tracts (II). Complementarily, in connectomic analysis, we expect to observe anatomically altered and microstructurally degraded ipsilesional hemispheric connectivity.

Methodology:

Population Selection:

All procedures and protocols for this study were reviewed and approved by the Colorado MultiInstitutional Review Board (COMIRB 17-1136). Subjects included in this study were patients who underwent resective surgery from January to December 2016 at the University of Colorado Hospital, to remove an intracranial tumor classified by histopathology as glioma requiring functional imaging due to localization in or near language or motor cortex. Metastatic tumor patient data (used for objective 2 only) were gathered from several secondary locations, also confirmed by histopathology and required functional imaging due to localization in or near language or motor cortex. Patient demographics, tumor diagnosis, and tumor lobe localization were collected retrospectively from patient chart review. For objective 1 and 2 (hemispheric and glioma grade analyses), subject population consisted of the heterogenous population of low- and high-grade gliomas (n=17). For objective 2 (tumor type analysis), subject population consisted of both heterogenous population of low- and high-grade gliomas (n = 17) as well as metastatic tumor (n = 7). For objective 4, the glioma population was screened for tumors localized in either the frontal or parietal lobes (n = 13). For objectives 3, 5, and 6 the glioma population was screened for viability for volumetric, ATA and connectometry analyses (n = 13). Two cases were removed due to tumor infiltration of the contralateral hemisphere. One case was removed due to tumor localization within the ventricle, which prevented any tracts from running through the tumor region of interest (ROI). One case was removed due to insufficient CST fibers traversing the tumor ROI, rendering it ineligible to contribute to the II experimental group. Due to time restraints, proof of concept for connectometry analysis was done on gliomas localized in the temporal lobe (n =2). Table 1 lists all tumor data.

Table 1

Glioma vs. Metastasis	Lobe Location	Diagnosis	Volume (mm³)
Glioma	Frontal	Grade IV Glioblastoma	30549
Glioma	Frontal	Grade IV Glioblastoma	45926
Glioma	Frontal	Grade IV Glioblastoma	49926.8
Glioma	Frontal	Grade III Astrocytoma	7468.2
Glioma	Frontal	Grade II Oligodendroglioma	4888.44
Glioma	Frontal	Grade II Oligodendroglioma	41332.6
Glioma	Frontal	Grade II Xanthoastrocytoma	15834.9
Glioma	Frontal	Grade II Glioma	16214.4
Glioma	Parietal	Grade IV Glioblastoma	14370.7
Glioma	Parietal	Grade IV Glioblastoma	14243.3
Glioma	Parietal	Grade IV Glioblastoma	27852.1
Glioma	Parietal	Grade III Oligodendroglioma	33484.8
Glioma	Parietal	Oligodendroglioma	5934.39
Glioma	Temporal	Grade IV Glioblastoma	145209
Glioma	Temporal	Grade IV Glioblastoma	53431.5
Glioma	Temporal	Grade III Astrocytoma	439.395
Glioma	Temporal	Grade II Astrocytoma	60055
Metastasis	Frontal	Adenocarcinoma	49973.4
Metastasis	Frontal	Carcinoid tumor	11766.4

Metastasis	Parietal	Amyloidoma	4139.87
Metastasis	Parietal	Amyloidoma	8319.37
Metastasis	Temporal	Esophageal Adenocarcinoma	6566.75
Metastasis	Occipital	Breast Cancer	4863.28
Metastasis	Occipital	Mucinous Adenocarcinoma	27184.6

Imaging sequence parameters:

Magnetic resonance images (MRI) were collected on a 3.0 T GE Signa scanner. MRI parameters were the following: T1-weighted image, T2-weighted-Fluid-Attenuated-Inversion-Recovery image (T2 FLAIR), field of view (FOV) 24 cm, TR: 9.5; flip angle: 20°. DTI – 1 b-value at 1000, 32 directions, axial FOV 24 cm, slice thickness 2.6 mm, spacing 0, frequency direction R to L, TR: 15, 500, 50 slices, phase/frequency 128, bandwidth 250, phase acceleration 2.0.

Pre-processing:

Tumor Segmentation:

For all cases, the tumor region was manually segmented using ITK-Snap using either preoperative T1-weighted or T2 FLAIR MRI scans as templates depending on which template provided optimal acuity of tumor boundary. All necrotic, hypoxic, and tumorigenic tissues (visible as hyperintensities on T2-FLAIR) were included in the segmentations. Final segmentations were verified by expert neurosurgical assessment (Dr. David Ryan Ormond). Figure 1 shows two representative segmentations using T2-FLAIR templates.

ITK-Snap Segmentation registration to DTI Image Space:

Original preoperative T1-weighted or T2 FLAIR images and ITK-Snap segmentations were registered to its respective 32 sampling direction image sets and b0 image on DSI (diffusion spectrum imaging) Studio (Yeh *et al.*, 2013). Figure 1B and 1D show the registered T2 and 3D segmentations of two cases to its respective DTI image space.

DSI Studio Streamline Deterministic Fiber Tracking:

Tractography reconstruction was conducted in DSI Studio (<http://dsi-studio.labsolver.org>). Complete 3D DTI image was reconstructed from patient 32 sampling direction image sets and respective b0 image (1000). This approach was done through DtiStudio, a program used by DSI Studio to compute diffusion tensor and reconstruct fiber bundles. DSI Studio also corrected for eddy currents and echo planar imaging (EPI) distortions. Eddy currents are the product of rapidly changing magnetic fields which can generate unwanted artifacts in MRI, such as blurring and spatial misregistration. EPI is how DTI is typically acquired, but irregularities between the 32 direction images and the b0 images cause image distortions. Following image reconstruction and correction, DSI Studio was used to run Streamline (Euler) Fiber tracking algorithm on the preprocessed preoperative DTI images. Whole-brain-seeding, CST and SLF fiber pathways were found using the Automated Anatomical Labeling Atlas and JHU White Matter Atlas to automatically define 3D ROIs (explained in detail below). DTI diffusion metrics AD, RD, MD, and FA were collected for all reconstructed fibers. The FA map (map which encodes the strength and direction of water diffusion for a given x, y, and z coordinate of the brain) and tract length of the CST and SLF were saved for each case and used for ATA.

Hemispheric ROI and tractography constructions and analysis:

The Automated Anatomical Labeling Atlas (AAL) was used to autosegment L/R hemisphere ROIs. Fiber tracking for the ipsilesional hemisphere was done by defining the hemisphere ipsilateral to the tumor as an ROI and the contralateral hemisphere as a region of avoidance (ROA). Fiber tracking for the contralesional hemisphere required defining the hemisphere contralateral to the tumor as an ROI and the hemisphere ipsilateral to the tumor as an ROA. Fiber tracking parameters in DSI Studio were all set to default. Raw values of tract number, AD, RD, MD, and FA were collected for both contralesional and ipsilesional groups. Normalization for each parameter was done using the following equation:

$$(i) = [x(i) - \min(x)] / [\max(x) - \min(x)]$$

where $x(i)$ represents the i th raw parameter value. Normalized tract data was plotted, and significance was calculated. Glioma grade comparison and glioma vs metastasis plots required the following equation to find normalized percent difference in tract parameter data:

$$\left(\frac{[\text{Normalized tract parameter value of ipsilesional hemisphere} - \text{Normalized tract parameter value of contralesional Hemisphere}]}{\text{Average normalized value of tract parameter}} \right) \times 100$$

Targeted white matter bundle reconstruction:

The John Hopkins University White Matter (JHU-WM) atlas was used to define L/R CST and SLF white matter tract ROIs. Fiber tracking was done using specific recipes of ROIs and ROAs: 1.) Contralesional (C): ROI- contralesional hemisphere WM bundle (CST or SLF); ROA- ipsilesional hemisphere. 2.) Ipsilesional Exclusive (IE): ROI- ipsilesional hemisphere WM bundle; ROA- contralesional hemisphere and tumor segmentation. 3.) Ipsilesional Inclusive (II): ROI- ipsilesional hemisphere WM bundle and tumor segmentation; ROA- contralesional hemisphere.

For all fiber tracking recipes, tracking parameters were set to DSI Studio default with the exception of seed termination (set to 50000). Tract length, AD, RD, MD, and FA were then collected and analyzed.

Volumetric Analysis:

Tumor volume (cm³) was collected for each case from ITK-SNAP manual tumor segmentation. Whole brain volume was calculated using volbrain (an online volumetry system)(Manjón *et al.*, 2016). For each case, tumor volume was normalized with the following equation:

$$([\text{cm}^3 \text{ tumor tissue} / \text{cm}^3 \text{ total brain tissue}] \times 100 = \% \text{ tumor volume})$$

and correlated to percent difference in mean diffusion metric:

$$(\{[\text{Mean diffusion metric of ipsilesional hemisphere} - \text{Mean diffusion metric of contralesional hemisphere}] / \text{Mean diffusion metric of whole brain}\} \times 100).$$

Lobe Localization Analysis:

Glioma cases were categorized under frontal, parietal, temporal, or occipital depending on tumor location. Parameters were set to distinguish between tumors near the frontoparietal border. The MRI slice containing the largest brain area was identified and measured vertically (anterior to posterior length). A horizontal line was drawn across the midpoint of the vertical measurement. >50% of the mass anterior to this line was classified as frontal and >50% of the mass posterior to this line was classified as parietal. Due to insufficient sample size for temporal and occipital cases, these gliomas were excluded from statistical analysis. AD, RD, MD, and FA were collected and

percent difference in mean diffusion metric were plotted with respect to targeted white matter bundle (CST or SLF) and glioma localization (Frontal or Parietal).

Along-Tract-Analysis:

For fibers extracted using the JHU-WM ROI seed-based approach for the CST and SLF, we computed the mean tract length across subjects, clustering the bundles into C, IE, or II groups. Using the mean tract length, a spline interpolation was applied to the x, y, and z coordinates of the fiber representation. Interpolation was used to resample the tracts and fit them to the standard mean length. Proximity of the CST and SLF fibers of the ipsilesional hemisphere to the tumor boundary was calculated. The tracts of the contralesional hemisphere were overlaid onto the ipsilesional hemisphere as a standard of comparison.

Structural Connectometry:

Connectivity matrix for temporal lobe localized gliomas (n=2) was calculated in DSI Studio (<http://dsi-studio.labsolver.org>). The AAL atlas was utilized for node reconstruction, and end-point count (number of tracts which terminate in a given brain area) was determined for all nodes of both hemispheres. Raw change in end-point termination from the contralesional hemisphere was calculated and plotted:

(ipsilesional count – contralesional count = raw change).

Results:

Objective 1: Glioma impact on hemispheric tractography

Preliminary analysis compared white matter tract number and diffusion parameters between the ipsilesional versus contralesional hemispheres (n=17) (Figure 2). The ipsilesional

hemisphere exhibited a significant increase in DTI derived fibers than the contralesional hemisphere ($p = 0.05$, $t = 2.02$, $df = 16$). All four diffusivity measures also showed significant differences on the ipsilesional compared to the contralesional hemisphere. RD, AD and MD showed an increase (RD, $p = 0.0012$, $t = 3.92$, $df = 16$; AD, $p = 0.02$, $t = 2.43$, $df = 16$; MD, $p = 0.003$, $t = 3.47$, $df = 16$), whereas FA showed a decrease (FA, $p = 2.51e-05$, $t = -5.84$, $df = 16$).

Objective 2: Glioma grade and metastasis impact on white matter integrity

Given the diversity of glioma grade present in our data set, we sought to determine whether different grades of glioma differentially impacted global white matter structure. We compared the normalized percent difference of same parameters between Grade II and Grade III/IV gliomas ($n=17$). It is well established that Grade III/IV gliomas exhibit more aggressive, invasive, and rapid growth compared to Grade II (Ormond *et al.*, 2017, Saini *et al.*, 2018). However, we observed no differences for any tract parameter between the Grade II and the more aggressive Grade III/IV gliomas (tract number, $p = 0.58$, $Z = 99$; RD, $p = 0.4$, $Z = 101$; AD, $p = 0.26$, $Z = 83$; FA, $p = 0.52$, $Z = 76$; MD, $p = 0.66$, $Z = 89$; Figure 3A). Our complete subject pool also contained a small population of metastasis patients ($n = 7$). Metastases are tumors which have developed from a tumor cell which broke off from a pre-existing tumor and traveled to a new location in the body. The following analysis compared ipsilesional tractographic impact from gliomas versus metastasis (Figure 3B). Similar to glioma grade comparison, there were no significant differences in normalized percent difference in tract number or diffusivity parameters between metastasis and glioma (tract number, $p = 0.89$, $Z = 215$; RD, $p = 0.12$, $Z = 188$; AD, $p = 1$, $Z = 202$; FA, $p = 0.28$, $Z = 195$; MD, $p = 0.16$, $Z = 235$).

Objective 3: Tumor volumetric correlation

A subsequent correlation was run between the percent volume of tumor vs the percent change in diffusion metric (n=13) (Figure 4). AD ($p= 0.86$, $r= -0.05$) and FA ($p= 0.92$, $r=-0.03$) showed a non-significant, negative correlation. RD ($p= 0.95$, $r= 0.02$) showed a non-significant, positive correlation. MD ($p= 0.99$, $r= 0$) showed no correlation.

Objective 4: Glioma lobe localization and its effect on the SLF and CST

In Figure 5A and 5B, we directly compared the impact of lobar localization of glioma on degradation in the CST and SLF with respect to the frontal and parietal lobes (n=13). For all diffusivity parameters, we observed no difference in the extent of impact on the CST when comparing between gliomas localized to parietal or frontal lobes (FA, $p = 0.66$; MD, $p = 0.34$; AD, $p = 0.37$; RD, $p = 0.35$; Figure 5A1-4). However, the SLF in parietal lobe localized glioma cases exhibited a significant increase in percent difference of mean AD, MD and RD compared to the SLF of gliomas localized in the frontal lobe (FA, $p = 0.06$; MD, $p = 0.03$; AD, $p = 0.04$; RD, $p = 0.03$; Figure 5B1-4).

Objective 5: Impact of glioma proximity on white matter integrity of CST and SLF

Boxplots were created showing the distribution of FA and MD between the three experimental groups, C, IE, and II, for both the CST and SLF (n=13) (Figure 6A-D). Comparison between experimental group diffusion metrics for the CST and SLF was done using a Kruskal-Wallis H-test (a non-parametric ANOVA). Post-hoc Dunn's test analysis was conducted for comparisons between experimental groups if H-test reached significance ($p<.05$).

CST Kruskal-Wallis H-test showed significant difference in distribution for FA and MD (CST FA $H(2)=8.46$, $p = 0.0145$; CST MD $H(3)=9.557$, $p = 0.0084$). Post-Hoc analysis for CST

FA and MD showed that II tracts had a significant decrease in FA and significant increase in MD compared to both C and IE tracts (CST FA: C v II $p= 1.005 \times 10^{-4}$; IE v II $p= 1.81 \times 10^{-4}$; CST MD: C v II $p= 7.3 \times 10^{-6}$; IE v II $p= 1.81 \times 10^{-3}$). No significant differences were seen in FA or MD of the CST between C v IE (CST FA: C v IE $p= 0.708$; CST MD: C v IE $p = 0.68$).

SLF Kruskal-Wallis H-test showed significant difference in distribution for FA and MD (SLF FA $H(2)=6.233$, $p = 0.044$; SLF MD $H(2)=19.004$, $p = 7.46 \times 10^{-5}$). Post-Hoc analysis for SLF FA showed that II tracts had a significant decrease in FA and a significant increase in MD compared to both C and IE (SLF FA: C v II $p= 0.003$; IE v II $p= 1.81 \times 10^{-6}$; SLF MD: C v II $p= 1.23 \times 10^{-7}$; IE v II $p= 0.008$). A significant increase was also observed in IE MD compared to C, which was not expected and may have resulted from a large distribution in IE data (SLF MD: C v IE $p= 0.03$). No significant differences were seen in SLF FA between C v IE (SLF FA: C v IE $p= 0.702$).

ATA was conducted for the CST and SLF (Figure 7B and Figure 7C). All tract lengths were normalized across subjects and plotted on the x axis in relation to distance from tumor boundary. Normalized FA and MD for C, IE, and II groups were plotted on the y axis. For the CST and SLF, we observe a decrease in FA in the II tracts specifically within the tumor boundary compared to the C tracts. We also observe preservation of FA as distance increases from the tumor boundary. This is seen through the decrease in metric difference between the C and II tracts, as well as the overlapping of the II and IE confidence intervals (indicated in black on the x axis) farther away from the boundary. MD analysis showed very similar results with an increase in MD and earlier overlapping of confidence interval between II and IE.

Objective 6: Glioma impact on structural connectivity

Figure 8 connectomes show the raw change in structural connectivity from the contralesional hemisphere for temporal lobe localized gliomas (n=2). Larger raw changes in end-point termination for a given node is represented by a larger area on the connectogram. With respect to the ipsilesional hemisphere, we observed a higher number of nodes which exhibited an increase in end-point termination compared to decreased end-point termination for both cases. We also observed certain nodes which consistently show an increase/decrease across both cases. For example, the 'Insula' and 'FrontalSup', among others, show a consistent pattern of increased connectivity and magnitude of increase in both cases. However, we observed that the increased connections may not be terminating in the same destination node. For example, the 'Insula' in Case 1 shows an increase in connectivity to the 'Postcentral' node, while the 'Insula' in Case 2 shows an increase in connectivity to the 'TemporalPoleSup' and 'Precentral' nodes. No statistical tests were run due to time restraints.

Discussion:

DTI is a valuable asset in the operating room, providing non-invasive white matter visualization which aids in maximal healthy tissue preservation (Bucci *et al.*, 2013). The goal of this study was to further explore DTI's capabilities as a pathophysiological tool, specifically addressing the feasibility of non-invasive study and diagnosis of gliomas and enhanced tumor border differentiation. Results indicated that these pathophysiological features can be derived through utilization of diffusion parameter analysis, ATA, and structural connectometry.

In this study, we used a hemispheric analysis to compare the contralesional hemisphere to the experimental ipsilesional hemisphere. A significant increase was observed in tract number,

RD, AD, and MD and significant decrease was observed in FA in the ipsilesional hemisphere (Figure 2). This is indicative of higher water diffusion radially (RD), less water restriction (MD), and weaker directionality (FA). This trend of decreased integrity has been seen in previous studies, providing evidence for DTI's consistency as proxy for axonal health (Ormond *et al.*, 2017, Clark *et al.*, 2012, Song *et al.*, 2003). This analysis also showed an increase in AD, indicating less axonal damage, similar to studies by Ormond *et al.*, 2017 and Racine *et al.*, 2014. This draws doubts on whether AD is truly measuring diffusion parallel to the tract or if tumor pathology increases diffusivity in all directions. This hypothesis would be consistent with the increase in RD and MD and decrease in FA since tracts would not exhibit high diffusion directionality. The increase in tract number was also surprising. An abnormal brain growth originating from the brain (non-metastatic) is expected to push surrounding tissue, resulting in an expected decrease in tract number (Ormond *et al.*, 2017). However, DTI analysis observes a significant increase in tract number, possibly due to brain re-wiring and compensation for decreased white matter integrity. Though AD and tract number are future areas of study, the three other measures show DTI metrics can be used to indirectly analyze and quantify pathological effect on white matter tractography.

Confirmation of differential diffusion between the ipsilesional and contralesional hemispheres, with the ipsilesional showing higher signs of white matter degradation, led to the question: do glioma grade and tumor type exhibit specific diffusion characteristics? Glioma grade analysis found no significant differences in normalized percent change of tract parameter between Grade II versus Grade III/IV gliomas (Figure 3A). However, a trend was observed in several parameters. Grade III/IV gliomas exhibited higher RD on the ipsilesional hemisphere compared to Grade II. Grade III/IV gliomas also showed a trend of lower change in AD and lower FA on the ipsilesional hemisphere compared to Grade II gliomas. This means the ipsilesional hemisphere of

higher-grade gliomas show higher radial diffusion, increase in axial diffusion (though it is not as high as axial diffusion found in Grade II), and lower FA compared to the ipsilesional hemisphere of Grade II gliomas. These are all consistent with higher signs of white matter structural degradation and is expected from a more aggressive grade of glioma (Ormond *et al.*, 2017, Saini *et al.*, 2018). Similarly, glioma ipsilesional impact versus metastasis ipsilesional impact showed no significant difference, but trends were observed (Figure 3B). Metastases exhibit higher ipsilesional RD (compared to gliomas) while gliomas induce lower ipsilesional FA and higher ipsilesional MD (compared to metastasis). These results hint that glioma grades and distinct tumor types may exhibit unique tractographic impact and DTI has the ability to non-invasively detect these exclusive pathophysiological characteristics. An increase in sample size may help bring these subtle trends to light.

Stemming from the previous analysis, we wanted to control for the impact that tumor volume might have on our results. We examined whether tumor volume was associated with the extent of white matter degradation and could potentially explain the trends seen in the grade and tumor type analyses. Percent tumor volume was correlated to percent difference in diffusion metric (I v C) (Figure 4), however no correlation was found between volume and change in diffusion metric. This suggested that the magnitude of decrease in white matter structural integrity observed on the ipsilesional hemisphere was not related to glioma volume and ruled out tumor volume as a confounding variable in the previous analyses.

To home in on the extent of glioma affects, we analyzed if the lobar localization of gliomas differentially impacted degradation of major white matter pathways (CST and SLF). In other words, does frontal lobe glioma localization differentially impact the fibers of the CST/SLF compared to parietal lobe localization. The results showed that, in the case of the CST, lobar

location did not affect the extent of impact of glioma (Figure 5A1-4). CST anatomical circuitry spans the frontal and parietal lobes, so it was expected that localization in either lobe would show similar extent of degradation. However, in the case of the SLF, we found that gliomas which arise in the parietal lobe have a higher negative impact on white matter integrity, with regards to increased (less restricted) water diffusion (increased RD, MD, and AD), than gliomas localized in the frontal lobe (Figure 5B1-4). The majority of SLF anatomical circuitry lies, and is most dense, in the parietal region. This is consistent with the results observed since glioma localization in the parietal lobe would impact more tracts of the SLF than a glioma localized in the frontal lobe.

The next question which stemmed from the lobar localization results was how does glioma effect vary with distance? Once again, these analyses were done on the CST and SLF. To begin tackling this question, we split tracts of the ipsilesional hemisphere into two experimental groups: IE and II. The contralesional (C) tracts were used as a control. Our hypothesis stated that the glioma impact would be localized to II tracts. Initial box plot analysis showed that II tracts showed higher signs of white matter degradation than C and IE tracts while IE had similar degradation patterns to C (Figure 6). This finding suggested that glioma impact is localized to the tracts which only cross through the tumor ROI, which led to the question does glioma impact span the entire length of II tracts or only the area of the tract within the ROI. ATA was used to answer this question (Colby *et al.*, 2012). Figure 7A shows a 3D visualization of a representative CST case in three anatomical planes. ATA was run on this case and normalized FA magnitude is indicated in the color bar. II tracts had a purple to yellow color scheme while IE tracts had a blue to yellow color scheme. Tracts outside the dark grey tumor ROI, from both IE and II groups, show higher signs of white matter health indicated by a lighter teal to yellow color, while tracts within the ROI boundary exhibit lower FA, indicated by dark purple. This observation lead to the hypothesis that ATA will

show glioma affect is limited to the area of the tract that is within the glioma. Figure 7B and 7C supported the hypothesis. White matter degradation was higher in II tracts limited to within the tumor boundary, as observed by the significant decrease in FA and increase in MD to the left of the vertical dashed line (demarcating the tumor boundary). We also observe similar normalized values of FA and MD for all groups past the tumor boundary. These findings indicate tumor effect on II tracts are localized to the tumor region.

Finally, the beginning phases of structural connectometry were done to show a proof of concept. Previous DTI studies have shown that gliomas shift white matter pathways in the brain (Ormond *et al.*, 2017, Gao *et al.*, 2017). However, no studies have holistically explored the glioma altered connectome. Results showed that the ipsilesional hemisphere contained nodes with increased and decreased connections and some of these nodes stayed consistent in both cases. Statistical analyses need to be conducted on a higher sample population to confidently locate which node pathways are consistently shifting due to glioma location. Pathophysiologically, this would provide a quantitative anatomical explanation for functional loss in glioma cases.

Broader impacts:

This research has several broader impacts and will spur new research questions. DTI has been an asset in the operating room, improving preoperative planning and intraoperative resection (Essayed *et al.*, 2017). Just recently DTI has been explored as a pathophysiological tool, taking the first steps towards non-invasive tumor diagnosis and study and better defining tumor borders. Few studies have used DTI as a diagnostic tool to classify glioma grade based on the effects these tumors have on surrounding white matter FA (Davarian *et al.*, 2017). In addition to diagnostic analyses, the level of axonal infiltration by glioma has been studied using DTI (Price *et al.*, 2003). More recent studies have expanded on this by exploring how gliomas affect white matter integrity

with regard to FA, MD, and ADC (Apparent Diffusion Coefficient) (Ormond *et al.*, 2017, Mori *et al.*, 2002). These studies have helped provide insight on the various capabilities of DTI in examining tumor pathophysiology. This project further examined the information which could be extracted from DTI tumor/white matter analysis data by addressing the limitations of previous studies, which included having a larger sample size, analyzing tract number, AD and RD along with the standard DTI measures, examining tract length anatomy with ATA, and exploring anatomical connection shift with structural connectometry. Preliminary analyses also show the potential for DTI to identify differential white matter degradation patterns between different glioma grades and tumor diagnoses. This future study has the potential to replace ex vivo, histopathology dependent diagnoses with in vivo, non-invasive DTI analysis. This study also brings us a step closer to reliably defining the tumor border to maximize glioma surgical resection. We show white matter distance plays a role in glioma effect, and that effect is highly localized to within the tumor boundary. This information and novel application of ATA can be used to aid accuracy in defining the tumor edge preoperatively and safely carrying out resection while maximally preserving normal tissue. Finally, DTI based connectometry can be a valuable asset in studying tumor pathophysiology. Glioma impacted connectomics provides a quantitative anatomical basis for functional loss due to glioma location, something gross histopathology cannot achieve. These quantitative measures would be achieved not only through the end-point analysis (as seen in this study), but also FA and MD analysis of these connections (measuring the overall white matter integrity of the connections between nodes). Surgeries can incorporate this information in preoperative planning and pay specific attention to these “at risk” pathways (lower structural integrity/decreased connections) intraoperatively.

Limitations:

This study comes with several limitations which should be improved upon in future experiments. The first was a limited subject population which was further restricted due to contralateral hemispheric infiltration by the tumor or atypical tumor origin. The analyses required patients with hemispherically isolated tumors so as to have within-subject controls (using the contralesional hemisphere). Increasing the number of subjects with hemispherically isolated tumors would potentially bring subtler tractographic patterns to light, such as the trends observed in the glioma grade (Figure 3A) and glioma versus metastasis analyses (Figure 3B). A second limitation of this study was the glioma impacted brain anatomy which resulted in tract shift. This complicated accurately locating the SLF on the ipsilesional hemisphere. Though guidelines for highlighting the SLF ROI was consistent for all cases, using established anatomical landmarks to highlight regions which the SLF pass through (Kamali *et al.*, 2014), brain shift should be taken into account when interpreting SLF analyses as it may have added or removed tracts from the SLF ROI. A lack of histopathological confirmation for each patient is also a limiting factor in this study. Individual histopathology would have provided a direct anatomical reference for the findings presented in this study. Furthermore, AD should be analyzed for what physiological response it is measuring. Though it very well could be measuring diffusion parallel to axons, there seems to be some doubt in the community regarding this metric (Ormond *et al.*, 2017, Racine *et al.*, 2014). Further studies establishing AD will allow for more confident interpretation of the metric in pathological cases, improving DTI's pathophysiological standing. Finally, time constraints restricted complete connectometry analysis. Future connectomic studies should focus on incorporating a larger sample size of hemispherically isolated tumors in the frontal, parietal, temporal, and occipital lobes. FA and MD analysis should also be incorporated to assess structural

integrity of these connections. These routes can back the use of DTI connectometry analysis in surgical settings.

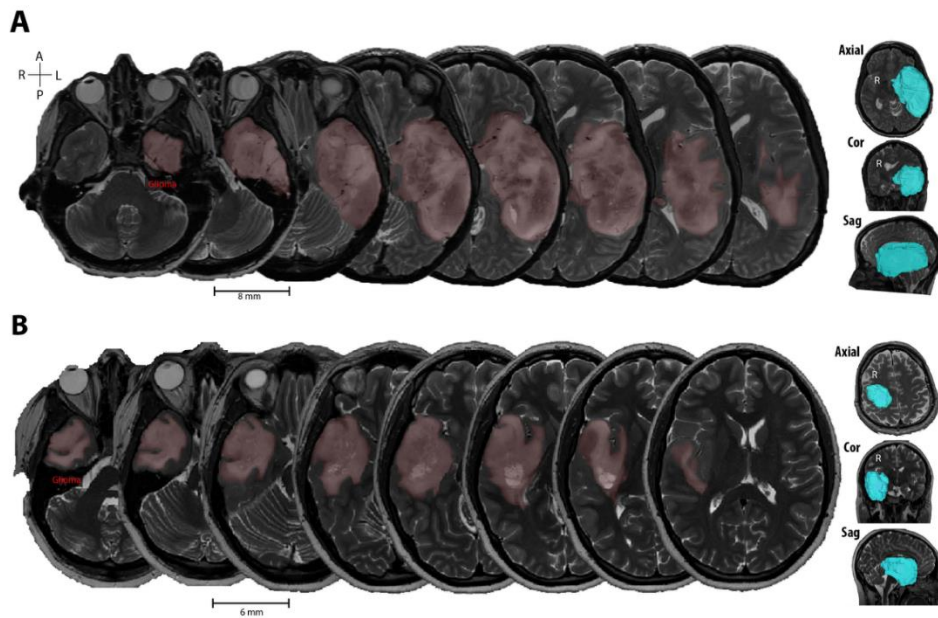
References:

1. Ostrom QT, Gittleman H, Truitt G, Boscia A, Kruchko C, Barnholtz-Sloan JS. CBTRUS Statistical Report: Primary Brain and Other Central Nervous System Tumors Diagnosed in the United States in 2011–2015. *Neuro Oncol* (2018) **20**:iv1-iv86. doi:10.1093/neuonc/noy131
2. Louis DN, Perry A, Reifenberger G, von Deimling A, Figarella-Branger D, Cavenee WK, Ohgaki H, Wiestler OD, Kleihues P, Ellison DW. The 2016 World Health Organization Classification of Tumors of the Central Nervous System: a summary. *Acta Neuropathol* (2016) **131**:803–820. doi:10.1007/s00401-016-1545-1
3. Goldbrunner R, Ruge M, Kocher M, Lucas CW, Galldiks N, Grau S. The treatment of gliomas in adulthood. *Dtsch Arzteblatt Online* (2018) doi:10.3238/arztebl.2018.0356
4. Raza SM, Lang FF, Aggarwal BB, Fuller GN, Wildrick DM, Sawaya R. Necrosis and Glioblastoma: A Friend or a Foe? A Review and a Hypothesis. *Neurosurgery* (2002) **51**:2–13. doi:10.1097/00006123-200207000-00002
5. Hervey-Jumper SL, Berger MS. Role of Surgical Resection in Low- and High-Grade Gliomas. *Curr Treat Options Neurol* (2014) **16**: doi:10.1007/s11940-014-0284-7
6. Treatment for Gliomas | Johns Hopkins Glioma Center. Available at: https://www.hopkinsmedicine.org/neurology_neurosurgery/centers_clinics/brain_tumor/center/glioma/treatment.html [Accessed March 3, 2019]
7. Deighton RF, McGregor R, Kemp J, McCulloch J, Whittle IR. Glioma Pathophysiology: Insights Emerging from Proteomics. *Brain Pathol* (2010) **20**:691–703. doi:10.1111/j.1750-3639.2010.00376.x
8. Alexander AL, Lee JE, Lazar M, Field AS. Diffusion tensor imaging of the brain. *Neurotherapeutics* (2007) **4**:316–29. doi:10.1016/j.nurt.2007.05.011
9. Winklewski PJ, Sabisz A, Naumczyk P, Jodzio K, Szurowska E, Szarmach A. Understanding the Physiopathology Behind Axial and Radial Diffusivity Changes-What Do We Know? *Front Neurol* (2018) **9**:92. doi:10.3389/fneur.2018.00092
10. Bucci M, Mandelli ML, Berman JI, Amirbekian B, Nguyen C, Berger MS, Henry RG. Quantifying diffusion MRI tractography of the corticospinal tract in brain tumors with deterministic and probabilistic methods. *NeuroImage Clin* (2013) **3**:361–368. doi:10.1016/J.NICL.2013.08.008
11. Essayed WI, Zhang F, Unadkat P, Cosgrove GR, Golby AJ, O'Donnell LJ. White matter tractography for neurosurgical planning: A topography-based review of the current state of the art. *NeuroImage Clin* (2017) **15**:659–672. doi:10.1016/j.nicl.2017.06.011
12. Caverzasi E, Hervey-Jumper SL, Jordan KM, Lobach I V., Li J, Panara V, Racine CA, Sankaranarayanan V, Amirbekian B, Papinutto N, et al. Identifying preoperative language tracts and predicting postoperative functional recovery using HARDI q-ball fiber

- tractography in patients with gliomas. *J Neurosurg* (2016) **125**:33–45. doi:10.3171/2015.6.JNS142203
13. Meyer EJ, Gaggl W, Gilloon B, Swan B, Greenstein M, Voss J, Hussain N, Holdsworth RL, Nair VA, Meyerand ME, et al. The Impact of Intracranial Tumor Proximity to White Matter Tracts on Morbidity and Mortality: A Retrospective Diffusion Tensor Imaging Study. *Neurosurgery* (2017) **80**:193–200. doi:10.1093/neuros/nyw040
 14. D’Andrea G, Familiari P, Di Lauro A, Angelini A, Sessa G. Safe Resection of Gliomas of the Dominant Angular Gyrus Availing of Preoperative FMRI and Intraoperative DTI: Preliminary Series and Surgical Technique. *World Neurosurg* (2016) **87**:627–639. doi:10.1016/j.wneu.2015.10.076
 15. Vassal F, Schneider F, Nuti C. Intraoperative use of diffusion tensor imaging-based tractography for resection of gliomas located near the pyramidal tract: comparison with subcortical stimulation mapping and contribution to surgical outcomes. *Br J Neurosurg* (2013) **27**:668–675. doi:10.3109/02688697.2013.771730
 16. Colby JB, Soderberg L, Lebel C, Dinov ID, Thompson PM, Sowell ER. Along-tract statistics allow for enhanced tractography analysis. *Neuroimage* (2012) **59**:3227–3242. doi:10.1016/j.neuroimage.2011.11.004
 17. Ormond DR, D’Souza S, Thompson JA. Global and Targeted Pathway Impact of Gliomas on White Matter Integrity Based on Lobar Localization. *Cureus* (2017) **9**:e1660. doi:10.7759/cureus.1660
 18. Natali AL, Bordoni B. *Neuroanatomy, Corticospinal Cord Tract*. StatPearls Publishing (2018). Available at: <http://www.ncbi.nlm.nih.gov/pubmed/30571044> [Accessed January 27, 2019]
 19. Kamali A, Flanders AE, Brody J, Hunter J V, Hasan KM. Tracing superior longitudinal fasciculus connectivity in the human brain using high resolution diffusion tensor tractography. *Brain Struct Funct* (2014) **219**:269–81. doi:10.1007/s00429-012-0498-y
 20. Hagmann P, Cammoun L, Gigandet X, Meuli R, Honey CJ, Wedeen VJ, Sporns O. Mapping the Structural Core of Human Cerebral Cortex. *PLoS Biol* (2008) **6**:e159. doi:10.1371/journal.pbio.0060159
 21. Hart MG, Ypma RJF, Romero-Garcia R, Price SJ, Suckling J. Graph theory analysis of complex brain networks: new concepts in brain mapping applied to neurosurgery. *J Neurosurg* (2016) **124**:1665–78. doi:10.3171/2015.4.JNS142683
 22. Bullmore E, Sporns O. Complex brain networks: graph theoretical analysis of structural and functional systems. *Nat Rev Neurosci* (2009) **10**:186–198. doi:10.1038/nrn2575
 23. Yeh F-C, Tseng W-YI. Sparse Solution of Fiber Orientation Distribution Function by Diffusion Decomposition. *PLoS One* (2013) **8**:e75747. doi:10.1371/journal.pone.0075747

24. Manjón J V., Coupé P. volBrain: An Online MRI Brain Volumetry System. *Front Neuroinform* (2016) **10**:30. doi:10.3389/fninf.2016.00030
25. Saini J, Gupta PK, Sahoo P, Singh A, Patir R, Ahlawat S, Beniwal M, Thennarasu K, Santosh V, Gupta RK. Differentiation of grade II/III and grade IV glioma by combining “T1 contrast-enhanced brain perfusion imaging” and susceptibility-weighted quantitative imaging. *Neuroradiology* (2018) **60**:43–50. doi:10.1007/s00234-017-1942-8
26. Clark KA, Nuechterlein KH, Asarnow RF, Hamilton LS, Phillips OR, Hageman NS, Woods RP, Alger JR, Toga AW, Narr KL. Mean diffusivity and fractional anisotropy as indicators of disease and genetic liability to schizophrenia. *J Psychiatr Res* (2011) **45**:980–8. doi:10.1016/j.jpsychires.2011.01.006
27. Song S-K, Sun S-W, Ju W-K, Lin S-J, Cross AH, Neufeld AH. Diffusion tensor imaging detects and differentiates axon and myelin degeneration in mouse optic nerve after retinal ischemia. *Neuroimage* (2003) **20**:1714–22. Available at: <http://www.ncbi.nlm.nih.gov/pubmed/14642481> [Accessed February 8, 2019]
28. Racine AM, Adluru N, Alexander AL, Christian BT, Okonkwo OC, Oh J, Cleary CA, Birdsill A, Hillmer AT, Murali D, et al. Associations between white matter microstructure and amyloid burden in preclinical Alzheimer’s disease: A multimodal imaging investigation. *NeuroImage Clin* (2014) **4**:604–14. doi:10.1016/j.nicl.2014.02.001
29. Davanian F, Faeghi F, Shahzadi S, Farshifar Z. Diffusion Tensor Imaging for Glioma Grading: Analysis of Fiber Density Index. *Basic Clin Neurosci J* (2017) **8**:13–18. doi:10.15412/J.BCN.03080102
30. Price SJ, Burnet NG, Donovan T, Green HAL, Peña A, Antoun NM, Pickard JD, Carpenter TA, Gillard JH. Diffusion tensor imaging of brain tumours at 3T: a potential tool for assessing white matter tract invasion? *Clin Radiol* (2003) **58**:455–62. Available at: <http://www.ncbi.nlm.nih.gov/pubmed/12788314> [Accessed March 4, 2019]
31. Mori S, Frederiksen K, van Zijl PCM, Stieltjes B, Kraut MA, Solaiyappan M, Pomper MG. Brain white matter anatomy of tumor patients evaluated with diffusion tensor imaging. *Ann Neurol* (2002) **51**:377–80. Available at: <http://www.ncbi.nlm.nih.gov/pubmed/11891834> [Accessed March 4, 2019]
32. Gao B, Shen X, Shiroishi MS, Pang M, Li Z, Yu B, Shen G. A pilot study of pre-operative motor dysfunction from gliomas in the region of corticospinal tract: Evaluation with diffusion tensor imaging. *PLoS One* (2017) **12**:e0182795. doi:10.1371/journal.pone.0182795

Figure 1:

**Figure 1:** Tumor segmentation and 3D rendering

Representative image of preoperative T2 FLAIR tumor segmentation to define tumor region of interest. Slice thickness of 8mm. 3D rendering of tumor segmented region by DSI-Studio is shown to the right.

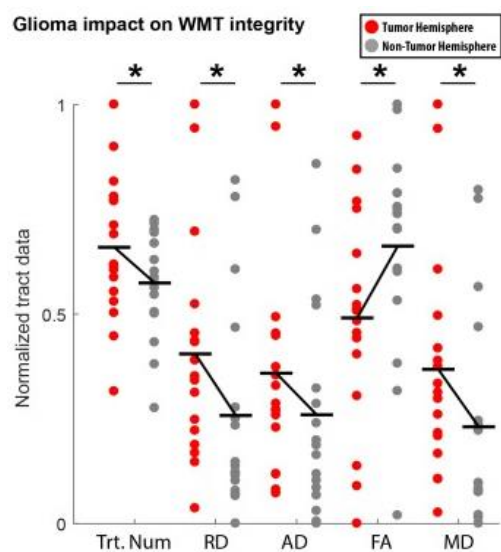


Figure 2: Glioma impact on white matter tract integrity

Comparison of global (hemisphere) white matter impact due to glioma using diffusivity parameters. Changes consistent with white matter degradation were observed on the ipsilesional hemisphere in RD (radial diffusivity), FA (fractional anisotropy), and MD (mean diffusivity).

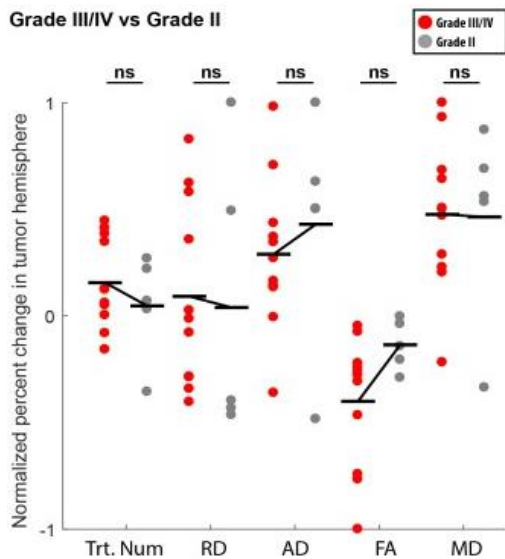


Figure 3A: Grade III/IV vs Grade II Glioma

Comparison of global (hemisphere) white matter impact due to high vs low grade glioma using diffusivity parameters. No differences were observed.

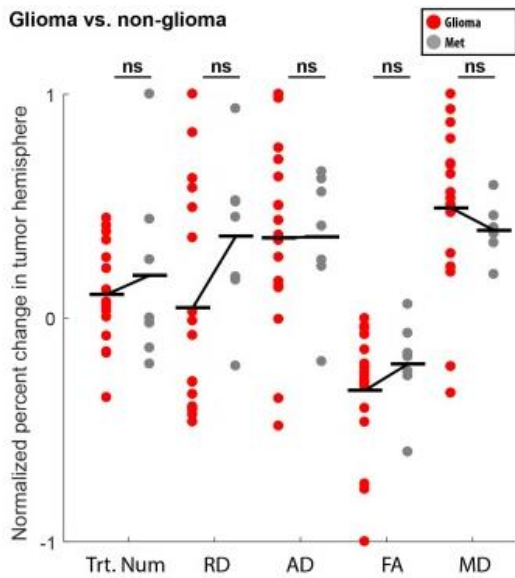


Figure 3B: Glioma vs. Metastasis

Comparison of global (hemisphere) white matter impact between glioma and metastasis using diffusivity parameters. No differences were observed.

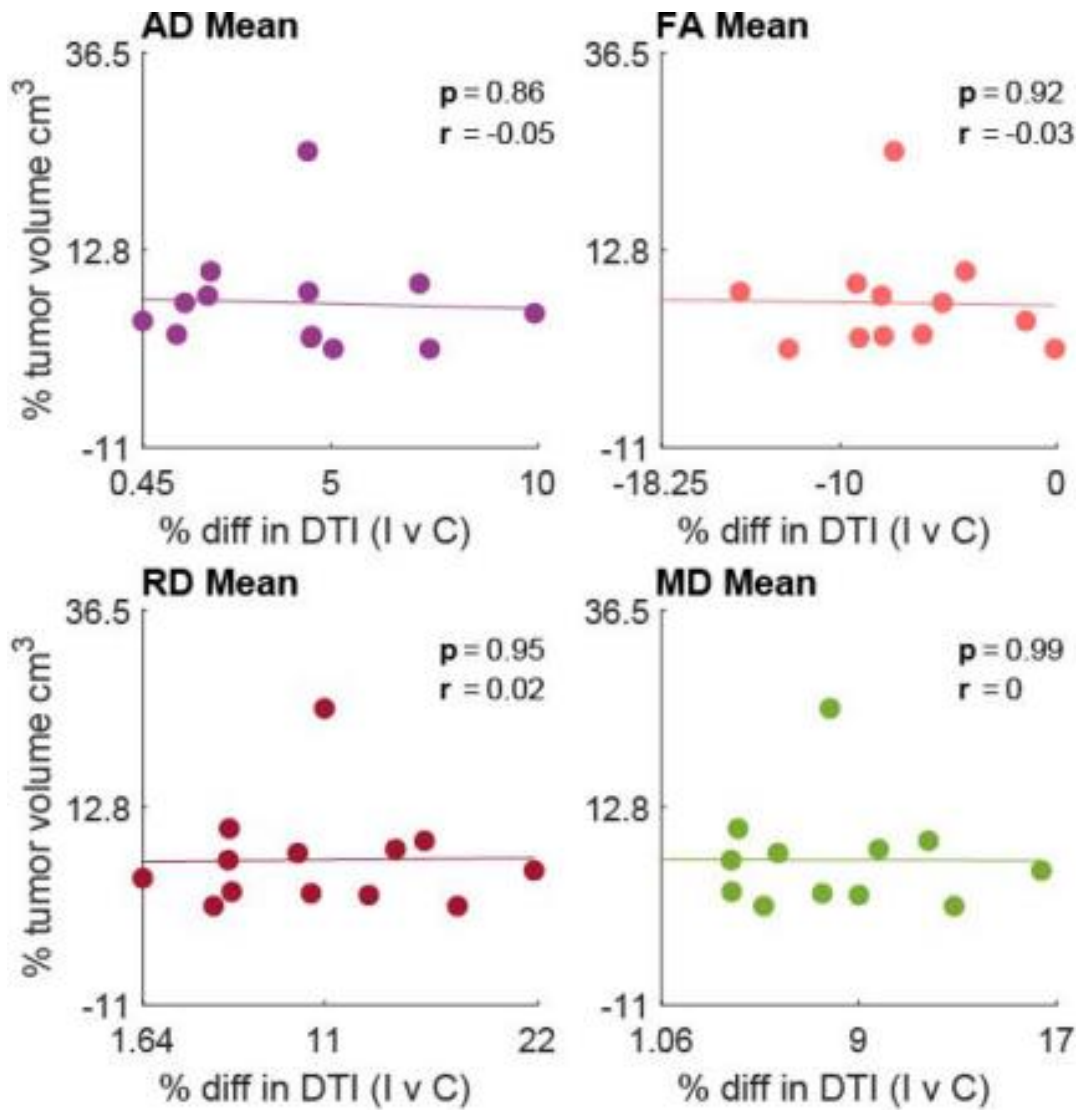


Figure 4: Tumor volume and diffusion metric correlation

Correlation between glioma volume and white matter impact for all diffusivity parameters. No correlational relationship was found for any parameter.

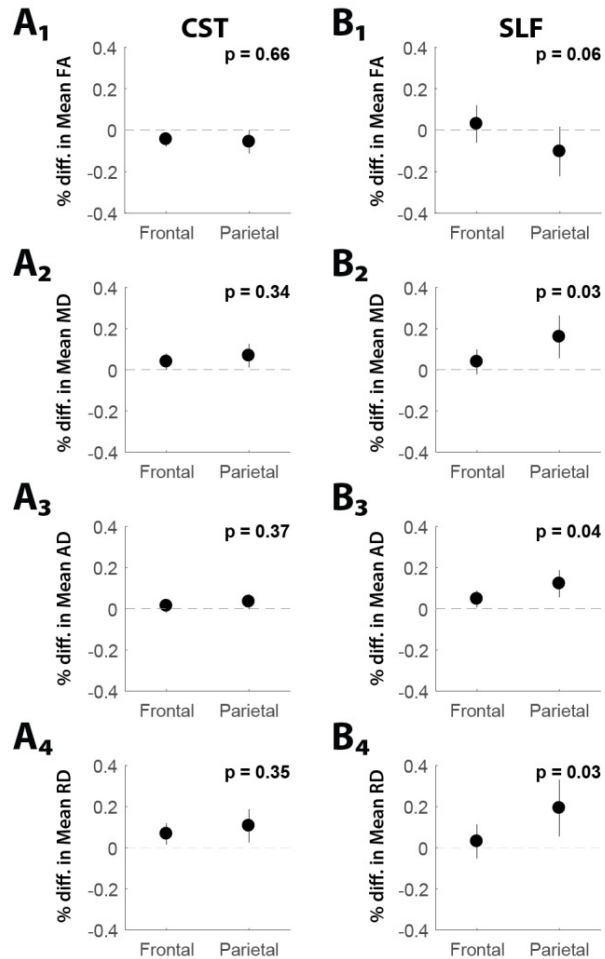


Figure 5: Impact of glioma lobar localization on major white matter architecture

(A1-4) Lobar location of glioma (i.e., frontal or parietal) did not differentially affect the white matter parameters of the CST (corticospinal tract).

(B1-4) Lobar location of glioma (i.e., frontal or parietal) had a significantly more negative impact on MD (mean diffusivity; B2), AD (axial diffusivity; B3) and RD (radial diffusivity; B4) of SLF (superior longitudinal fasciculus) white matter architecture

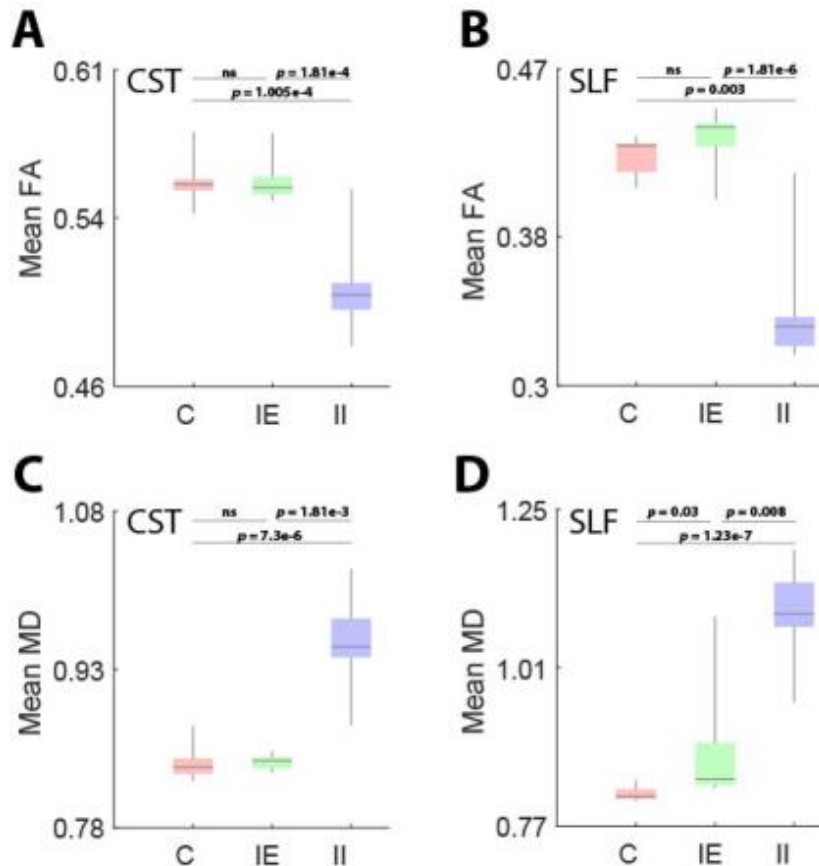


Figure 6: Impact of glioma on CST and SLF C, IE and II tractography

Boxplot analysis comparing the difference in mean FA and MD of CST (corticospinal tract)/SLF (superior longitudinal fasciculus) C (contralateral)(control), IE (ipsilesional exclusive) and II (ipsilesional inclusive) tractography. Results show a significant decrease in white matter structural integrity of II tracts compared to both IE and C tracts in terms of decreased FA and increased MD (6A-D). No significant difference in white matter structural integrity was found between IE and C groups (6A-C), excluding SLF Mean MD comparison (6D).

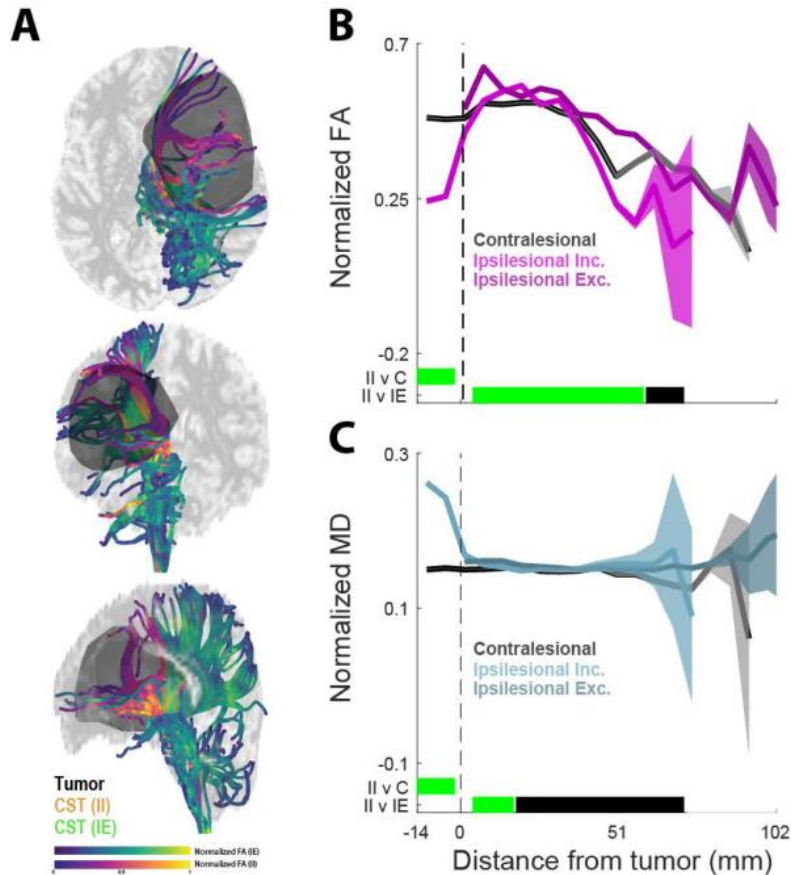


Figure 7: Impact of glioma distance on tractography using Along-Tract-Analysis

(7A) Representative CST (corticospinal tract) case in three anatomical planes. 3D rendering of tumor ROI (region of interest) is color coded in dark gray. FA (fractional anisotropy) of IE (ipsilesional exclusive) tractography is color coded in dark purple – teal – yellow and II (ipsilesional inclusive) tractography is color coded in dark purple – pink – yellow, both scales representing low to high FA respectively. Results show lower white matter health (lower FA) (dark purple) in tractography within and near the tumor ROI and higher white matter health (increased FA) (teal/pink - yellow) in tractography farther away from the tumor ROI.

(7B-C) ATA (Along-Tract-Analysis) point-by-point analysis along the distance of normalized tracts of the CST C, IE and II groups to determine localized difference in FA and MD. Results show a decrease in white matter structural integrity of II tractography limited to within the tumor border compared to the C and IE tractography.

Temporal lobe tumors

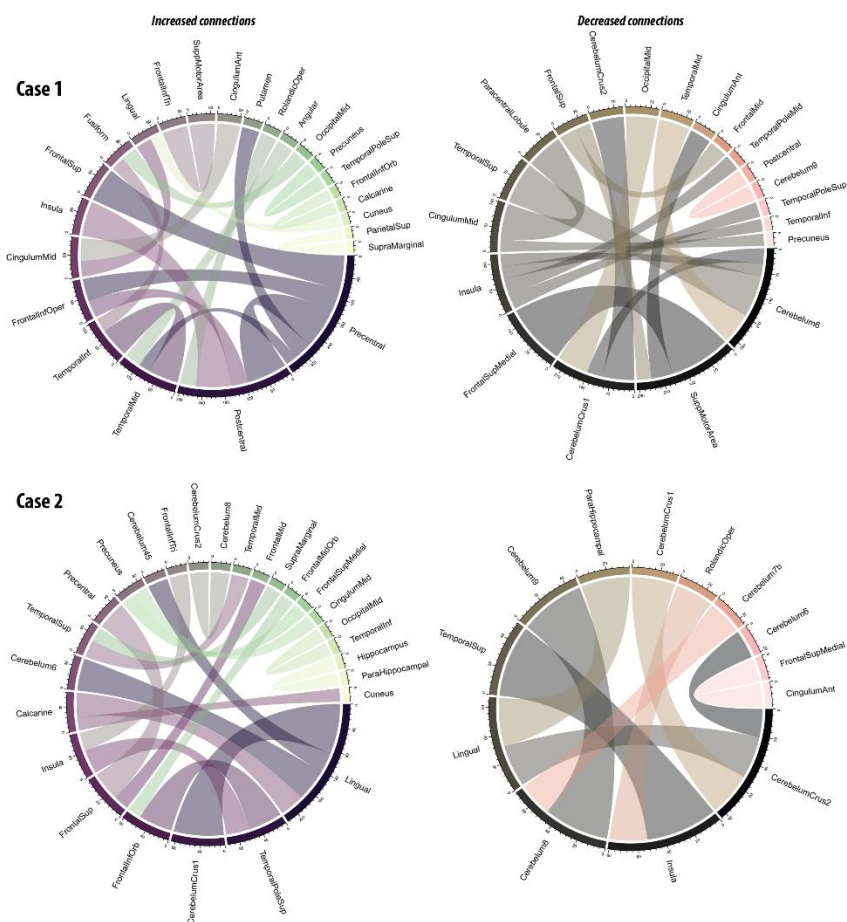


Figure 8: End-point connectograms of temporal lobe localized gliomas

Connectometry analysis depicting raw change in node connectivity with respect to the ipsilesional hemisphere. Increased node connections are shown on the upper and lower left and decreased node connections are shown on the upper and lower right. Area dedicated to the node on the connectogram is proportional to the magnitude of change. No statistical analyses were done on this data.